Proceedings of ASME Turbo Expo 2011
GT2011
June 6-10, 2011, Vancouver, British Columbia, Canada

GT2011-46303

ASSESSMENT OF NUMERICAL TOOLS FOR THE EVALUATION OF THE ACOUSTIC IMPEDANCE OF MULTI-PERFORATED PLATES.

A. Andreini, C. Bianchini, B. Facchini, F. Simonetti
Department of Energy Engineering "Sergio Stecco"
Via Santa Marta, 3 - 50139 Firenze, Italy
francesco.simonetti@htc.de.unifi.it

A. Peschiulli
AVIO Group s.p.a., Torino
Via I Maggio, 56 - 10040 Rivalta di Torino, Italy

ABSTRACT

Multi-perforated liners, commonly employed in Gas Turbine combustors as cooling devices to control metal temperature, are recognized as very effective sound absorbers. Thus, in the innovative lean combustion technology, where the onset of thermo-acoustic instabilities represents one of the most important issue, the multi-perforated plates can be exploited both for wall cooling and damping combustion instabilities.

As a first step of a large experimental and numerical research program regarding multi-perforated liners, an investigation of different numerical methodologies to analyze acoustic damping is here reported.

In particular three different numerical techniques to evaluate planar waves sound absorption of perforated plates are presented and validated with literature test cases. A quasi 1-D code, implementing the wall compliance concept, provides results for a large set of geometric and fluidynamic conditions. A large test matrix was investigated varying perforation hole angle and diameter with different overall porosities. The effect of bias and grazing flows Mach number was tested as well.

A subset of considered geometries were then supported by a full reconstruction of the unsteady pressure field by means of a Large Eddy Simulation computed with an open-source code. Non-reflective boundaries with forcing term provide the wave to acoustically excite the perforated plate. Multi-microphone post-processing technique allowed the reconstruction of a progressive and regressive planar wave to compute the reflection coefficient.

All results were cross-checked with a Finite Element Model, able to solve the wave equation in the frequency domain with a background velocity field.

NOMENCLATURE

A	absorption coefficient $1-\|R\|^2$	
a	spatial mode temporal coefficient matrix	
B	stagnation enthalpy	$[m^2/s^2]$
b	spatial mode temporal coefficient inverse matrix	
c	speed of sound	$[m/s]$
C	correlation matrix	
D	diameter	$[mm]$
f	frequency	$[Hz]$
h	plate thickness	$[mm]$
j	imaginary number	
K	Rayleigh's conductivity	
k	wave number	$[1/m]$
L	length	$[m]$
Ma	Mach number	
N_m	number of modes	
N_s	number of snapshot	
p	static pressure	$[Pa]$
P^+	progressive pressure wave	$[Pa]$
P^-	regressive pressure wave	$[Pa]$
Q	volume flow rate	$[m^3/s]$
R	reflection coefficient $\frac{P^-}{P^+}$	
RQL	Rich Quench Lean	
S_x	axial spacing	$[mm]$
S_y	tangential spacing	$[mm]$
St	Strouhal number	
t	time	$[s]$
U	velocity vector	$[m/s]$

V	plenum volume	$[m^3]$
x	spatial position	$[m]$
X	streamwise coordinate	$[m]$
Y	wall distance	$[m]$
Z	spanwise coordinate	$[m]$
Greeks		
α	hole inclination angle	$[^\circ]$
η	wall compliance	
ρ	density	$[kg/m^3]$
μ	dynamic viscosity	$[kg/ms]$
σ	porosity	$[\%]$
ϕ	velocity potential	$[m^2/s]$
ψ	velocity spatial mode	$[m/s]$
Γ	K real part	
Δ	oscillation amplitude	$[Pa]$
ω	angular frequency	$[rad/s]$
Supercripts		
d	downstream section	
k	generic mode	
u	upstream section	
$'$	fluctuating part	
$+$	dimensionless in viscous units, downstream propagating wave	
$-$	upstream propagating wave	
Subscripts		
b	bulk	
eff	effective	
h	hole	
i	generic vector component	
i, j	generic snapshot	
ref	reference value	
x	axial direction	
y	tangential direction	
∞	farfield values	
0	reference quantity	
bias	bias flow	
grazing	grazing flow	

INTRODUCTION

The onset of pressure fluctuations due to thermo-acoustic instabilities is a well-known issue of low NOx emissions gas turbine combustors based on lean premixed flames. Several theoretical and experimental studies have been carried out in the last years to help engineers in the prediction and control of such phenomena [1, 2], having as main result the definition of successful design practices for stable and highly operable land-based gas turbine combustors.

The expected future regulations concerning NOx emissions from civil aero-engines (ACARE Vision 2020 objectives and future ICAO-CAEP standards) have forced in the last ten years huge research investments from the main engine manufacturers to introduce lean burn combustion systems. Even though classical RQL technology has still relevant improvement potentials, with the expected next NOx reduction targets (up to 80% with respect to CAEP/2 standards) lean combustion will sooner or later be adopted by each manufacturer.

Despite the specific adopted solutions, lean burn aero-engine combustors are affected by thermo-acoustic issues, which need to be addressed in order to keep engine operations stable and safe. Combustion dynamics knowledge from land-based gas turbine combustors is being exploited but some fundamental improvements related to fuel effects and to the more stringent safety requirements are still necessary. In particular typical active control techniques are not suitable for aero-engine applications due to reliability issues. On the other hand, among common standard passive damping systems, large volume Helmholtz resonators are likely to heavily impact on overall engine size and they cannot be adopted. The most promising passive acoustic dampers seem to be the multi-perforated liners (such as effusion cooling) usually used to contain the combustion zone.

Multi-perforated liners are commonly used in gas turbines combustion systems to reduce wall temperature within limits established by mechanical characteristics of material. Common cooling systems, such as effusion and impingement are accomplished with a direct drilling of liner metal in the former case [3, 4], and with a second external perforated plate which provide cool jets pointing the cold side of liner in the latter case.

Both systems consist of arrays of small orifices through which a mean cooling air flow (generally named bias flow) is blown on the wall inside the combustor. The air streams on both sides of the perforated liner are subjected to thermo-acoustic fluctuations, even though the flow on the combustor side is prone to more intense oscillations. The resulting acoustic pressure difference across each hole forces a fluctuating air mass flow rate across it; this is superimposed on the mean flow of the jet of cooling air. The formation of vortices at the holes exit rims promote a viscous dissipation of incident acoustic energy, that can produce a broadband acoustic damping [5].

Therefore, the opportunity to use liner cooling holes design as a damping strategy to partially control pressure fluctuations must be investigated taking into account thermal requirements of liner material and the significant reduction of cooling air mass flow expected with the next generation of lean burn combustors.

Recent theoretical and experimental studies have examined and verified the damping potentials of multi-perforated liners. In particular it is worth to mention recent papers by Heuwinkel et al. [6] and Bhayaraju et al. [7].

In the first work a comprehensive experimental study about the influence of several geometric and fluidynamic parameters on damping performance of multi-perforated liners is reported. Relevant results are the confirmation of porosity as the key geometric parameter, with a negligible effect of holes number and diameter, and the presence of an optimum pressure ratio where

maximum damping performance is observed. The combination of these two relationships has a fundamental importance in the two-fold optimization of cooling-damping characteristics of the device.

In the paper by Bhayaraju et al. [7] an actual effusion cooled tubular combustor is considered. The purpose is the observation of the interaction between cooling air and the flame transfer function: it is reported a significant flame response variation increasing cooling air Mach number when normal holes are considered, while typical tilted film cooling holes are not observed to affect the flame, with an acoustic damping only slightly dependent on coolant Mach number.

Experimental surveys as the previously cited are certainly fundamentals steps towards the definition of affordable cooling-damping design rules, but typical industrial practices require the availability of accurate and reliable numerical tools both for fast preliminary geometry sizing and for final accurate verification.

The purpose of this work is the implementation and the assessment of a set of numerical models commonly used for the prediction of acoustic behavior of multi-perforated plates. The considered methodologies spread over three increasing levels of complexity.

The first is a one dimensional network model based on linear acoustics and on the generalization of Howe's Rayleigh conductivity. As reported in [6] and [7] this approach proved its capabilities even with complex geometries.

The second approach consists in the generalization of the first model to standard Finite Element methodology to solve 3D acoustic fields in the frequency domain with a superimposed mean flow field. In this work it will be explored the opportunity to characterize multi-perforated liner impedance in FEM acoustic solvers that nowadays probably represent the most viable tools for 3D computations of combustion instabilities on actual geometries [8, 9, 10].

Last methodology considered in this assessment work is Large Eddy Simulation (LES). The ability of LES to provide details about the flow field across multi-perforated plates and to predict the associated acoustic damping has been recently assessed by some authors [11, 12]. The results of a set of aeroacoustics LES computations concerning single periodic jet, with some discussions about considered numerical boundary conditions and post processing techniques, are reported in this paper. The effect of holes staggering was investigated and a modal analysis of the flow and pressure fields presented.

For each methodology a synthetic description of theoretical background will be outlined, followed by some details about selected or implemented numerical tools and by a description of comparative test case geometries.

METHODOLOGY

1D network tool

One-dimensional network tools based on linear acoustics and lumped parameters are reliable models widely used to quickly perform stability analysis and to compute resonance frequencies and modal shapes of thermo-acoustics systems such as gas turbine combustors. These models are typically developed in a modular approach so that blocks can be modified or added by the user to take combustor characteristic elements that can significantly alter system thermo-acoustics, such as flame models, resonators, inlet/outlet, etc., into account. The acoustic damping of multi-perforated liners should also be considered in the equivalent lumped 1D network in use. Such numerical tool, suitable for the investigation of longitudinal modes of gas turbine combustors, was previously implemented and described in [13].

The system is made up of cylindrical ducts, with an equivalent diameter comparing to the real system, having similar fluidynamic conditions to take into account for the mean velocity field. At both terminations ad-hoc boundary conditions are imposed; for the present investigation, semi-infinite boundaries are applied to avoid acoustic wave reflections. It relies on conservation equations formulated in terms of fluctuating stagnation enthalpy B' and velocity U'. The network solver was however lacking a dedicated module to include the impedance contribution of multi-perforated plates with bias flow.

For this purpose, a specific model based on linear acoustics in presence of planar waves was developed in the same MATLAB® environment. The damping of planar waves by perforated liners is treated following the mathematical formulation of Dowling and Eldredge [14] which is based on the definition of a wall compliance η, where the damping holes are treated as isolated holes, according to Howe [15] and Leppington [16]. Dowling and Hughes [17] extended the aforementioned concept to a regular pattern of holes, relating the overall wall compliance η to the Rayleigh's conductivity K [18]:

$$\frac{1}{\eta} = \frac{\pi D_h^2/4}{\sigma L^2 K} + \frac{t_{eff}}{\sigma L} \tag{1}$$

where the definition takes into account for the liner thickness as well, and:

$$K = -jkL\frac{Q'}{B'\,|_{0-}^{0+}} = \frac{D_h}{L}(\Gamma + j\Delta) \tag{2}$$

Γ and Δ are defined by Howe [15] as a function of the orifice Strouhal number $St = D_h\omega/(U_b/2)$.

The wall compliance was then implemented as a boundary condition in the specific acoustic element replicating the multi-perforated liner, according to the model described so far. Outside

the perforated liner a plenum with rigid walls was considered. In such a way the absorption coefficient A for the perforated liners was calculated in terms of an energy balance across the perforated liner:

$$A = 1 - \frac{B_d^{2+} + B_u^{2-}}{B_u^{2+} + B_d^{2-}} \tag{3}$$

FEM Acoustic Solver

Besides 1D network tools, other numerical approach capable of investigating thermo-acoustic behavior of real gas turbine combustors are available. Among them, the finite element approach is a reliable tool that allows to investigate 2D or 3D acoustic domains giving additional details on the pressure field, comparing to 1D tools.

In technical literature there are several examples of FEM techniques used to evaluate frequency response, eigenfrequencies and acoustic modes. Pankiewitz and Sattelmayer [8] investigated an annular combustor in presence of a fluctuating heat release in the time domain showing attractive FEM potentialities for a complete thermo-acoustic combustor description. Camporeale and Campa [9] made an investigation on a similar annular test case, focusing on eigenfrequencies and modal shapes below and above the first cut-on frequency. Both studies were performed with the commercial software COMSOL®Multiphysics. Following those successful applications, COMSOL®is here used to investigate multi-perforated liners. The acoustic module based on a frequency domain solver with a background mean flowfield, is here used to analyze all selected cases.

In the present context the fluid is assumed to be an ideal gas and the flow is compressible, inviscid and irrotational. With such hypothesis the simplified Navier-Stokes equations are solved in terms of the compressible velocity potential ϕ and in the frequency domain, the wave equation for the velocity potential $U = \nabla\phi$ becomes:

$$-\frac{i\omega\rho}{c^2}\left(i\omega\phi + U\cdot\nabla\phi\right) + \nabla\cdot\left[\rho\nabla\phi - \frac{\rho}{c^2}\left(i\omega\phi + U\cdot\nabla\phi\right)U\right] = 0 \tag{4}$$

where the acoustic pressure is given by:

$$p(x,t) = -\rho\left(i\omega\phi + U\cdot\nabla\phi\right) \tag{5}$$

The software is able to set the boundary conditions in terms of rigid wall, open exterior, radiation condition, PML (Perfectly Matched Layers) (see Hu et al. [19] and Hu [20] for a detailed description) or specific impedances Z. For the forcing boundary it's possible to set the fluctuating pressure in terms of velocity potential with an user-defined amplitude $\phi = \phi_0$ and the perforated liner impedance was defined according to wall compliance definition made in Eq. 1.

For all the investigated test cases the mesh element size was chosen so that $L_{mesh} \leqslant c/(3f)$ and before running the simulations, sensitivity was performed to verify the independence of solutions with respect to the generated mesh.

Large Eddy Simulations

In order to give a deep insight of the flow field developing around the holes of the plate, a full reconstruction of the unsteady turbulent structures is necessary. A set of Large Eddy Simulations was thus performed, to study both the free jet flow dynamics and the acoustic response of the excited jet in the linear regime. Such technique results to be highly expensive in terms of computational resources compared to the other numerical tools proposed: a fine spatial discretization is in fact needed on the three-dimensional domain to directly resolve at least partially turbulent fluctuations. The simulation of an entire perforated liner is unfeasible and also domains including several holes result to be very computationally expensive, not allowing extensive investigations in terms of flow and acoustic conditions. This paper is thus focused on studying a single periodic hole configuration with bias flow and orthogonal planar pressure wave excitation.

The open-source finite-volume toolbox OpenFOAM [21] was used, in particular a pressure based solver implementing time resolved PISO loop for compressible flow was exploited [22]. Time step was set constant to maintain maximum Courant number around 0.5. Equations were discretized with a second order centered scheme for the convective term and a backward implicit Euler scheme for time integration. Subgrid stresses were considered following the Smagorinsky approach with VanDriest near wall damping [23]; the Wall Adaptive Local Eddy-viscosity model by Nicoud [24] was also implemented to assess the near wall modeling sensitivity. Anyhow no sensible differences for the two SGS models was recorded and results are presented with no reference to the model in use. Near wall grid requirements for wall resolved LES ($Y^+ < 1$; $X^+ < 100$; $Z^+ < 40$) were satisfied clustering the grid close to the wall. A posteriori analysis were conducted in order to verify the far field grid requirements: the ratio of modeled to resolved turbulent kinetic energy is below 0.2 and the ratio of the filter width to the Kolmogorov length scale, estimated using subgrid dissipation, is below 10 everywhere in the domain.

Aiming at reproducing holes repeatability, periodic boundaries are imposed around the hole, respecting the axial and the tangential pitch and maintaining axis orthogonality thus implementing an ideally infinite array of jets.

Inlet and outlet boundaries were treated with adjustable partially and non reflecting boundary conditions known in literature as the Navier Stokes Characteristic Boundary Conditions [25]. A fully reflecting specified velocity boundary was set at the entrance while for the outflow a sinusoidal pressure was imposed

on a non reflecting boundary. With the aim of saving computational resources a multi-frequency excitation was implemented. Validation was performed against purely sinusoidal signals at selected frequencies (700, 1000 and 1300 [Hz]) providing a variation of the reflection coefficient less than 1%. Dual modes excitation were also tested showing the same level of agreement.

The acoustic response of the perforated plate was reconstructed following the multi-microphone post processing technique [26]. Instantaneous pressure was recorded at specific positions x_i for 30 excitation cycles of which only the last 20 were considered. Afterwards the signal was decomposed into a progressive and regressive wave, as specified in Eq.6, using a best fitting on phasors at the specified frequencies:

$$p(x_i,t) = \sum_k \left(P^+(f_k) \cdot e^{-j2\pi f_k/cx_i} + P^-(f_k) \cdot e^{j2\pi f_k/cx_i} \right) \cdot e^{-j2\pi f_k t}. \tag{6}$$

Such decomposition allows to easily compute the reflection coefficient R which is a complex number.

The Proper Orthogonal Decomposition (POD) post processing technique, reviewed for the analysis of turbulent flows in [27] and applied to measurements of naturally and acoustically excited jets in [28, 29], was also implemented to permit a modal analysis of the flow structures reproduced. Such technique projects the instantaneous solution $U_i(x)$ onto a time independent set of orthonormal basis functions $\psi^k(x)$, chosen as optimal in terms of projection error minimization. Temporal coefficients a_i^k describe the relative influence of the different spatial modes at the various times at which solution is recorded. Once decomposed, the unsteady flow field can be reconstructed using Eq.7.

$$U_i(x) = \sum_{k=1}^{N_m} a_i^k \cdot \psi^k(x) \tag{7}$$

To reduce computational costs of the procedure, the snapshot method [30] was selected to construct the basis functions and the temporal coefficients. From a given number of snapshots, the temporal coefficients are calculated as the eigenvectors of the correlation matrix C which is an $N_s \times N_s$ tensor constructed using a scalar product between the solution snapshots:

$$C_{ij} = U_i(x) \cdot U_j(x). \tag{8}$$

The basis functions can be finally computed as:

$$\psi^k(x) = \sum_{i=1}^{N_s} b_i^k \cdot U_i(x). \tag{9}$$

where the matrix b is the inverse of the time coefficient matrix a.

This technique can be applied also to other quantities, i.e. pressure or temperature, just redefining the scalar product in Eq.8 to compute the correlation matrix. Modes are usually arranged with decreasing corresponding eigenvalue.

VALIDATION TEST CASE

The numerical tools presented so far were validated against the experimental and numerical work of Bellucci et al. [31]. The same set of experimental data was used by Mendez and Eldredge [11] to validate a similar set of numerical models. The reference test is composed of a thin perforated screen with a bias flow and a normal to the screen acoustic wave confined in the linear regime. Main geometric parameters and flow conditions are reported in Tab.1.

Geometry		
$S_x = S_y$	35	$[mm]$
D_h	6	$[mm]$
σ	2.31	[%]
h	1.5	$[mm]$
Flow conditions		
U_b	5.0	$[m/s]$
T_∞	293.15	$[K]$
p_∞	100000	$[Pa]$
Δp	5	$[Pa]$

TABLE 1. **Geometric characteristics and flow conditions**

Results are reported in terms of absorption coefficient A and phase of reflection coefficient as function of excitation frequency. Simulations were performed with the numerical methodologies presented in the previous sections; results are also compared in terms of the standard Howe's model, that will be referred to as HM in the following, and the modified Howe's model (MHM) that accounts for liner thickness contribution.
As a general result, FEM and the 1D network-based tool gave identical results: accordingly, in Fig.1 results for the FEM and 1D tool overlap on the same curve.

As reported in Fig.1, the agreement between experiments and numerical predictions is substantially good for the absorption coefficient. All the investigations predict a very similar behaviour characterized by the presence of a maximum at which A is close to unity (the incident acoustic wave is almost completely

absorbed by the system) around 400 Hz. Concerning peak frequency LES computation slightly over-predicts such value while the FEM analysis is in under-prediction with respect to experiments. The correction for the plate thickness on Howe model is in this case not beneficial as the curve is shifted towards lower frequencies and predict a faster decrease of absorption after 400 Hz.

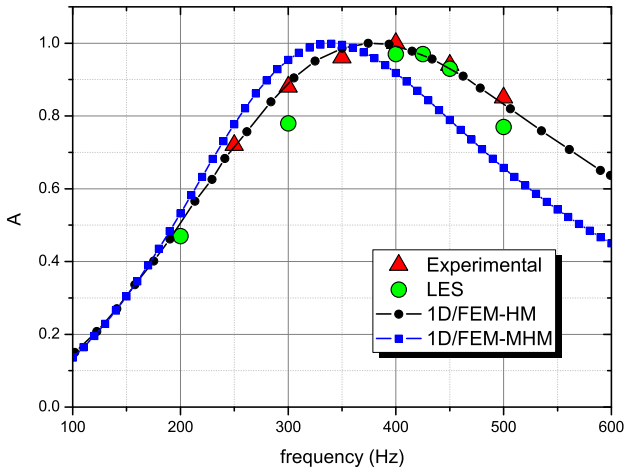

FIGURE 1. **Absorption coefficient - Bellucci test case**

Fig.2 plots the phase of reflection coefficient. First thing to note is the different behavior of LES predictions compared to both experiments and FEM analysis in the proximity of the maximum of the absorption coefficient. The change in sign of the phase occurs at the frequency at which the maximum of the absorption coefficient is located. Even though such frequency is quite well captured by the three computations, the LES code switch from a negative to a positive phase shift passing from $-\pi$ to π while the FEM computations progressively reduce the shift achieving zero corresponding to the maximum. When the absorption coefficient is almost unitary the regressive pressure wave amplitude is almost null and it is easier to mispredict the phase of such wave. Such trends were also reported in [11] for similar computations.

ACOUSTIC ANALYSIS OF MULTI-PERFORATED LINER

Geometric and Fluidynamic Test Matrix

In order to explore the damping behavior of realistic multi-perforated liners, a matrix of 9 different geometries was defined, taking into account various grazing and bias flow Mach numbers. A complete analysis of the entire test matrix was carried out with the 1D approach, while deeper investigations through LES and FEM methodologies were performed on a selected case.

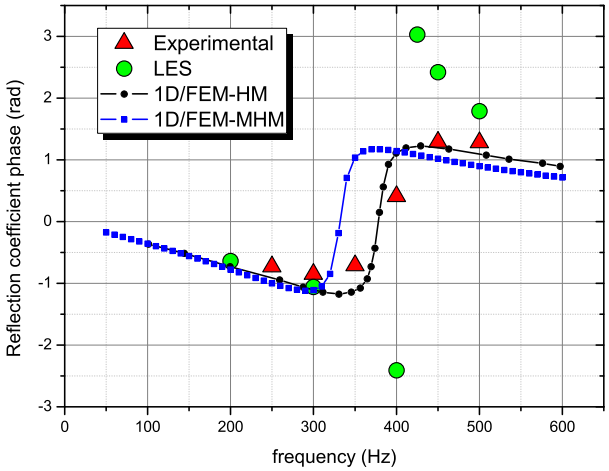

FIGURE 2. **Reflection coefficient phase - Bellucci test case**

Perforations have been applied to a cylindrical liner with an as-

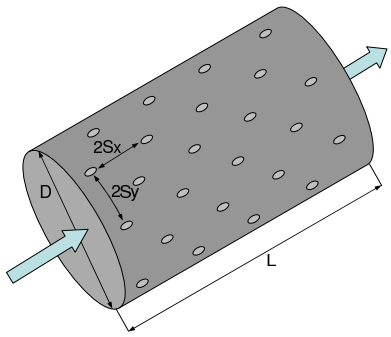

FIGURE 3. **Sketch of selected perforated liner geometry**

pect ratio $L/D = 1$ and a thickness h of 2.5 mm (see Fig.3). Each geometry consists of 18 equi-spaced staggered rows along the axial direction ($S_x = 7.3\,mm$) each with 72 holes in tangential direction ($S_y = 5.9\,mm$). Holes diameter D_h is varied from 0.8 to 1.2 mm, while considered holes tilting angles α are 30°, 60° and 90°. With three different holes diameter selected, correspondent levels of porosity σ are explored: 1.17, 1.82, 2.63 %. Having a regular drilling, porosity can, in this case, be computed as:

$$\sigma = \frac{0.25\pi D^2}{S_x \cdot S_y} \tag{10}$$

The grazing and bias flows effects were investigated, respectively, in the range $M_{grazing} = 0 - 0.1$ and $M_{bias} = 0 - 0.13$. Ge-

ometries and flow conditions are summarized in Table 2, where bold data refers to the case selected for LES and FEM analysis.

Geometry		
S_x	**7.3**	$[mm]$
S_y	**5.9**	$[mm]$
D_h	**0.8**-1-1.2	$[mm]$
α	30, 60, **90**	$[^\circ]$
σ	**1.17**-1.82-2.63	$[\%]$
h	**2.5**	$[mm]$
Flow conditions		
$M_{grazing}$	**0**-0.1	
M_{bias}	0-0.13 (**0.1**)	
T_∞	**293.15**	$[K]$
p_∞	**100000**	$[Pa]$

TABLE 2. Multi-perforated liner test matrix

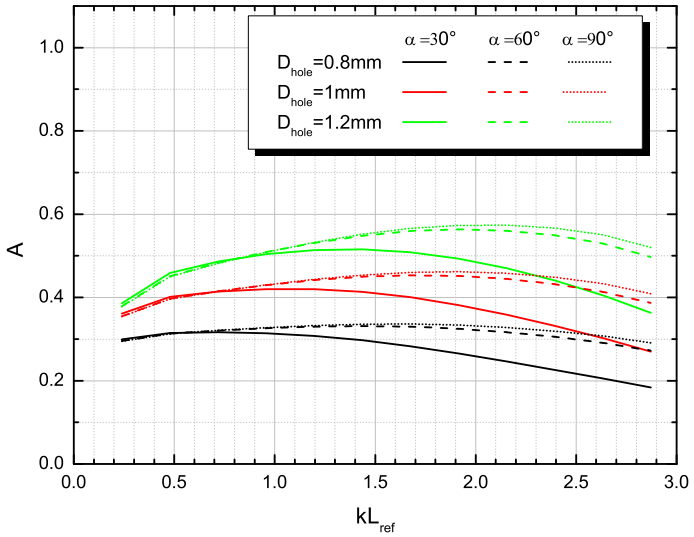

(a) $M_{grazing} = 0.1$ and $M_{bias} = 0.05$

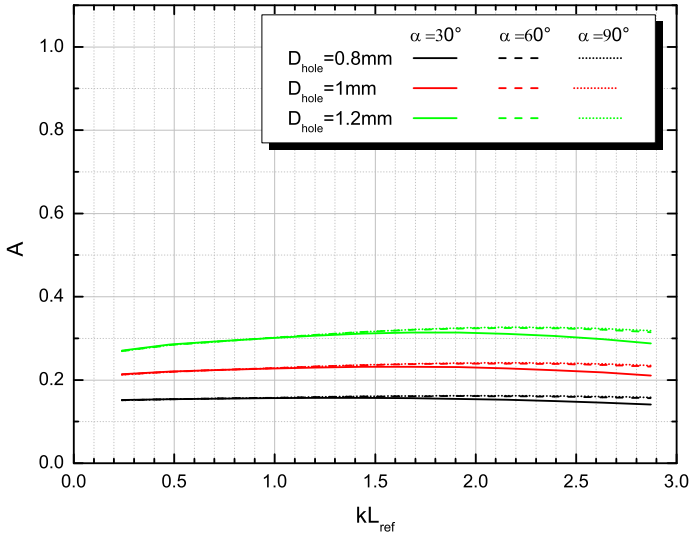

(b) $M_{grazing} = 0.1$ and $M_{bias} = 0.13$

FIGURE 4. **Absorption Coefficient - Sensitivity to Liner Overall Porosity and Hole Inclination Angle**

1D network tool predictions

The absorptive capabilities of all the 9 investigated geometries were evaluated with the 1D network tool in terms of the energy dissipation coefficient A defined in Eq. 3; for brevity reasons only a selection of obtained results will be presented.

First of all, the effect of the overall porosity was assessed by varying the hole diameter, and hole inclination angle was investigated for two different bias flow conditions and $M_{grazing} = 0.1$, representative of a real combustor mean flow; results are plotted in Figs. 4(a) and 4(b).

It is possible to point out a relevant effect of the liner porosity: with increasing values the absorptive capabilities of the multi-perforated liners are improved. Moreover lower bias flows are beneficial for absorption enhancement: comparing $M_{bias} = 0.05$ with $M_{bias} = 0.13$ results, the absorption nearly doubles. However the higher bias velocities are less frequency dependent so, in the planar wave range, liner response to variations of combustion instabilities excitation frequency is negligible.

The effect of hole inclination α is important as well: holes perpendicular to liner centerline show better absorption capabilities in the upper frequency range for the lower bias Mach number; in such conditions, the improvement of acoustic absorption is up to 50% with $D_h = 0.8mm$. From a numerical standpoint such effect is embodied within the wall compliance taking into account the effective liner thickness (Eq. 1). The effect is not linear increasing α from 30° to 90°, suggesting that good acoustic performance can be obtained with 60° as well.

In Figs. 5(a) and 5(b) results for two different hole inclination angles ($\alpha = 30^\circ$ and $\alpha = 90^\circ$) are plotted. As already pointed out, $M_{bias} = 0.03$ exhibits the higher absorption with both investigated porosities. For $\alpha = 30^\circ$, the maximum absorption with the smallest diameter, occurring at $kL_{ref} = 0.5$, is about

40% with the lower bias flow velocity. Decreasing with frequency it reaches the absorption calculated for higher bias flow at $kL_{ref} = 2$; same trend is confirmed also for the larger diameter. At $\alpha = 90^\circ$ an overall shift towards higher frequencies does not permit an equivalent reduction of absorption for the low bias flow within the investigated range of wave number.

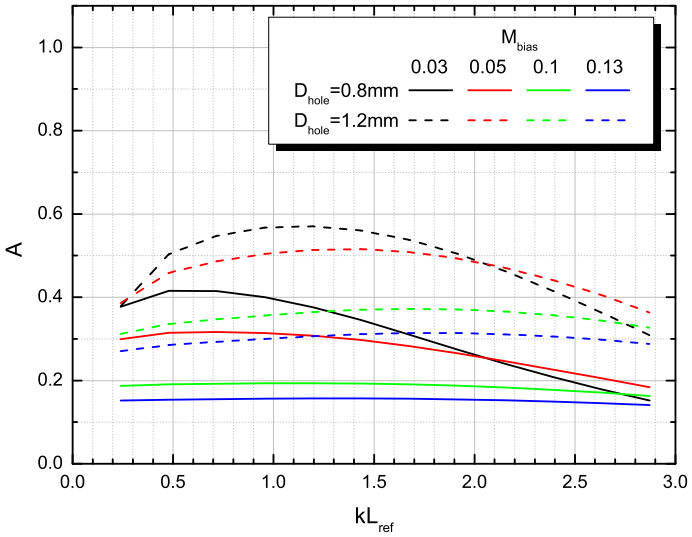

(a) $M_{grazing} = 0.1$ and $\alpha = 30^\circ$ Results

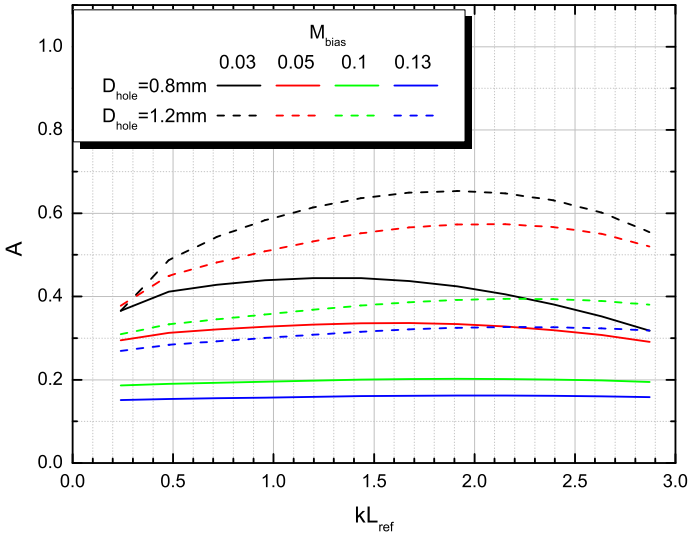

(b) $M_{grazing} = 0.1$ and $\alpha = 90^\circ$ Results

FIGURE 5. Absorption Coefficient - Sensitivity to M_{bias} and Liner Overall Porosity

Collecting all numerical predictions described so far, discussed results provide important information on the acoustic behavior of multi-perforated liners in real combustion chambers: as a general remark, the acoustic energy dissipation can be significantly improved by increasing the overall porosity with fixed fluidynamic conditions; such improvement also allows to shift the maximum absorption towards higher frequencies so that the liner has better energy dissipation characteristics over a wider frequency range. From a design standpoint, the increase of hole inclination is beneficial as well, specially in the upper frequency range with low bias velocities, showing a more uniform absorption over the investigated frequency range; this behavior counteracts cooling performances that can be better achieved with smaller hole inclinations. With $M_{bias} = 0.1$ and 0.13, that are closer to real working conditions, the improvement of absorption with perpendicular holes is practically negligible showing that optimal acoustic energy dissipation can be maintained also with highly inclined holes necessary to guarantee adequate cooling performance.

Besides geometrical parameters, the bias velocity has a key role in changing the overall absorption: up to $M_{bias} = 0.05$, the energy dissipation is frequency dependent and beneficial for the lower frequency regimes, as at engine part-load operation.

LES and FEM predictions
90° angle - in-line

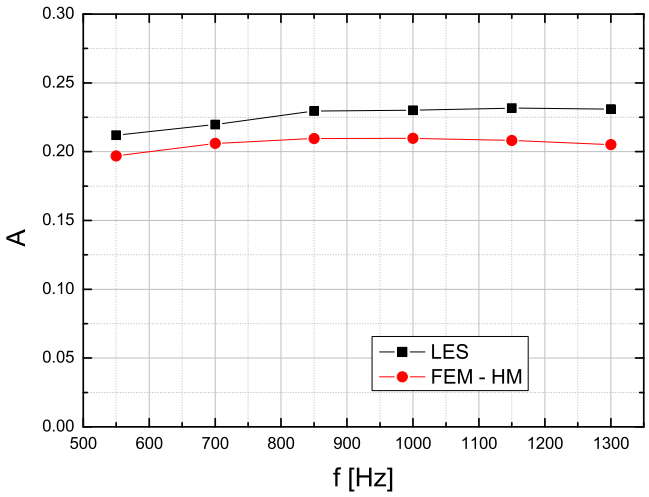

FIGURE 6. Absorption coefficient - LES predictions

A similar computation as the validation test, i.e. 90° angled in-line holes and no grazing flow, was performed at the flow conditions reported in Table 2 (bold data).

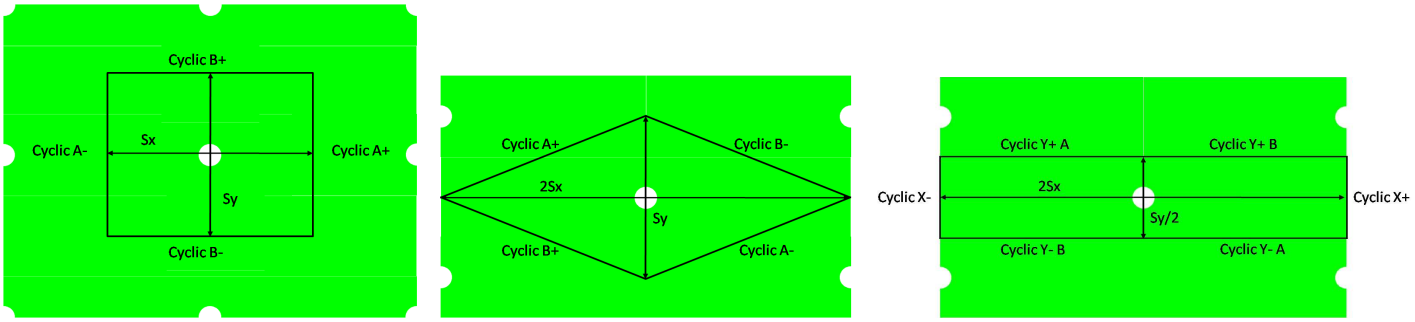

(a) In-line domain (b) Staggered Rhomboidal domain (c) Staggered Rectangular domain

FIGURE 7. Domain definitions

Regarding LES computations, the investigated range of frequencies is confined between 550 and 1300 [Hz] with steps of 150 [Hz]. Even though lower frequencies were of interest as well, the high computational cost of longer simulation periods are limiting at the moment the lower bound of investigated frequency range. Amplitude of excitation was differentiated, maintaining linear regime: from 114 to 126 [dB], for the various frequencies in order to maximise the decoupling of the multi-frequency excitation.

Concerning the computational costs a total period of 30 cycles at 500 [Hz] corresponds to 0.06 [s]. The computational grid, composed of nearly $7 \cdot 10^5$ cells, imposes a fixed time step of $5 \cdot 10^{-7}$ [s] to guarantee $Co < 0.5$ resulting in a total amount of 300000 iterations completed in 280 CPU hours circa on a quad core Intel Xeon X5472 at 3.00GHz.

The results obtained are reported in Fig.6 in terms of absorption coefficient against FEM predictions with standard Howe model. Both predictions do not show a strong dependency on frequency: all values are comprised between 0.2 and 0.25, with LES data resulting to be slightly higher than the acoustic finite element solver. The gap between the two analysis is growing with frequency, but results are to be confined around 10% and the trend is quite well reproduced.

90° angle - staggered

An attempt to investigate the effect of staggering was performed changing the domain and the periodicity definition. Fig.7 shows a comparison between the in-line arrangement in Fig.7(a) and two different approaches to cope with hole staggering. The first one implements a diamond shaped domain with standard cyclic boundaries on the corresponding side of the rhomboid, as depicted in Fig.7(b). In the second one, see Fig.7(c) the staggered condition is achieved doubling the distance of the stream-wise cyclics and halving the tangential one. Furthermore the tangentially periodic boundary is cut in two identical sectors and cross-paired. Experiences with the rhomboidal domain are reported in several works [12,32,33], however due to the high axial to tangential pitch ratio of this test case a set up based on the diamond domain would have created too highly skewed elements with an hexahedral mesh. The second approach was thus chosen by the authors to maintain highly orthogonal cells, and the inclusion of a grid refinement close to the stream-wise boundary was necessary in order to maintain a certain fitting in the two sides discretization.

The acoustic simulation to assess the effect of staggering was conducted at 1300 [Hz] and compared with equivalent analysis performed via the FEM code with standard Howe's model. The staggered holes reduce the absorption coefficient as predicted by both codes even though the LES predictions reveal a much stronger dependency of the holes arrangement. The higher absorption for the in-line configuration in fact is inverted into an under-prediction for the staggered arrangement.

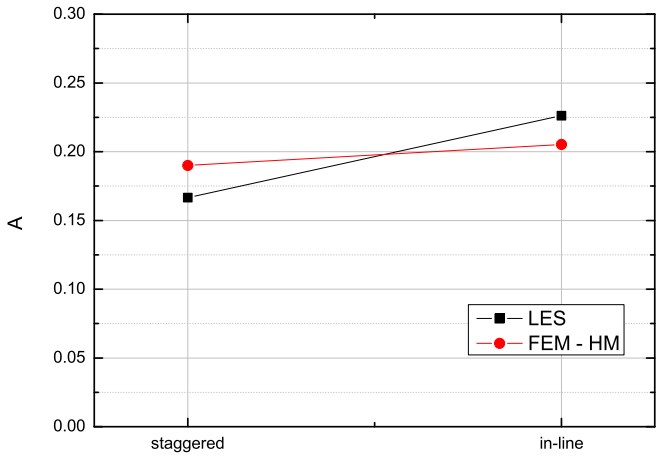

FIGURE 8. Absorption coefficient - Effect of staggering

FLOW FIELD ANALYSIS

In order to better understand the fluidynamic mechanism through which acoustic energy is dissipated across the hole, an analysis of the flow field of the naturally excited jet was performed taking advantage of the very high level of detail released by LES computations. This is relevant for the acoustic analysis, since the investigated range of forcing largely reside in the linear regime, as long as the selected frequencies are far from those associated with the natural modes of the jet.

An overview of the flow field on the symmetry plane is given in Fig.9 reporting a contour plot of the instantaneous and the mean axial velocity.

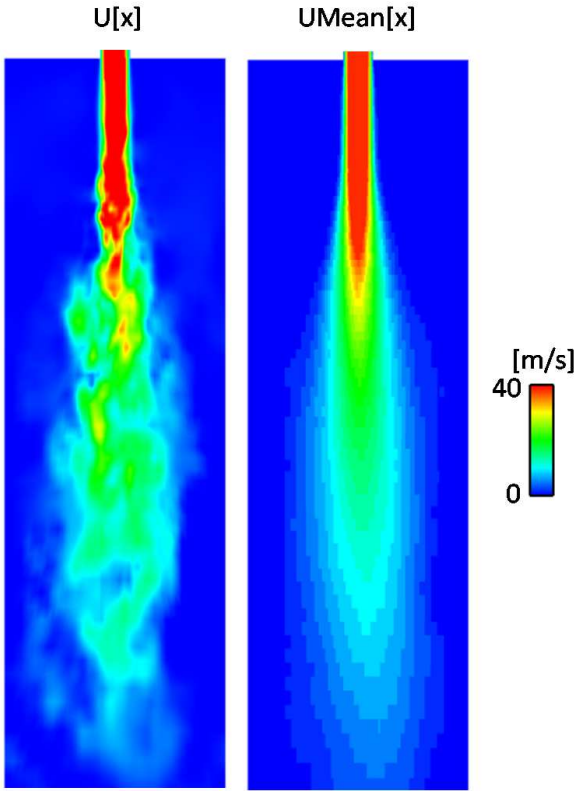

FIGURE 9. **Instantaneous and mean axial velocity - LES predictions**

Even though experimental data were not available to directly compare the numerical predictions, main flow structures of the free jet can be recognized in the instantaneous velocity field to validate the turbulent jet behaviour. Due to the long L/D ratio, no vena contracta can be appreciated in the potential core. Spatial resolution was not sufficient to directly resolve the Kelvin-Helmoltz instability structures developing on the margin of the potential core, anyhow turbulent transition and the progressive diffusion into a fully developed core is captured. The time averaged velocity plot is also shown in order to assess the mean extension of the jet inside the domain, small asymmetries in the profile are due to the shortness of the simulation period.

A modal analysis has been conducted to investigate the near hole flow more in detail. The region inside the box extending $2.5 \cdot D_h$ in the jet direction and $2 \cdot D_h$ in the span direction was selected to compute the Proper Orthogonal decomposition analysis. Both the velocity and pressure modes were investigated on 340 snapshots equally spaced in time over a period T= $4.08 \cdot 10^{-3}$ [s].

The velocity analysis results to be less spatially defined compared to the pressure one due to the interaction of the different velocity component on the same mode. First pressure modes are thus analyzed here and corresponding velocity modes are exploited to understand the flow field associated with the pressure mode themselves. Since the acoustic energy, corresponding to the pressure decomposition, and the kinetic energy, relative to the velocity analysis, are not equivalent, corresponding modes might be found in different positions. Spectral analysis and compatibility of pressure and velocity fields allowed to establish a connection between the most energetic, in both sense, modes.

The first mode is equivalent to the mean pressure field thus it is not presented. The following modes usually present equivalent but symmetric modes, for example mode 2 and 4 have inverse pressure distributions respectively at mode 3 and 5, not reported for the sake of brevity. Fig.10 shows the pressure distribution on the symmetry plane aligned with the axial pitch for modes 2 and 4. The corresponding velocity modes point out that those structures correspond to co-rotating and counter rotating vortices respectively on the same symmetry plane. Three dimensional isosurfaces reveal that mode 2 correspond to vortex rings aligned with the hole axis while mode 4 connects two misaligned co-rotating lobes on the two sides of the hole. The order of the corresponding velocity modes is inverted being respectively the 5th and the 3rd modes, meaning that the kinetic energy content is actually higher for the misaligned vortex rings.

The relative kinetic energy content is a fundamental parameter in order to estimate the weight of each mode in the global solution and how many modes are necessary to completely describe the flow. It was computed from the eigenvalue associated with the given velocity mode representing the energy contained in the mode itself. Fig.11 shows the relative fluctuating energy content of first 21 modes except the first, associated with the mean flow and thus excluded from the fluctuating energy computation. All these first 20 modes present an energy content above 1%, with first 6 modes ranging between 7 and 3.5%. These findings are in line with POD of experiments for a natural circular jet at Re = 6700 as reported in [28].

The temporal coefficients for modes 2 to 5 were later analyzed in order to assess the dominating frequencies by means of a Discrete Fourier Transform. The investigated range of frequen-

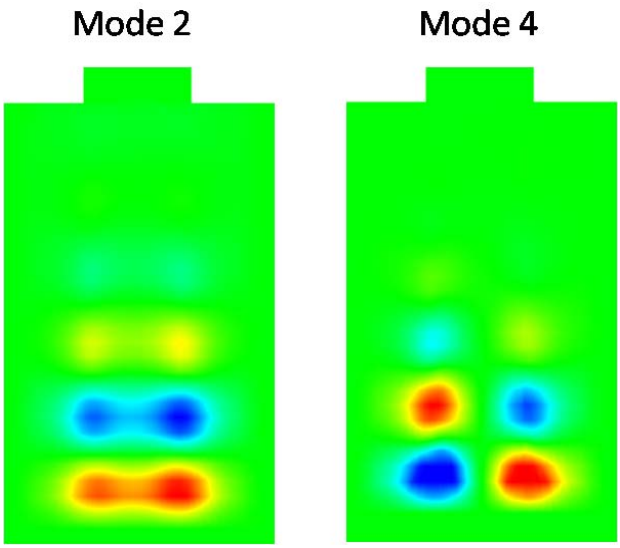

FIGURE 10. **Pressure POD modes 2 and 4 - LES predictions**

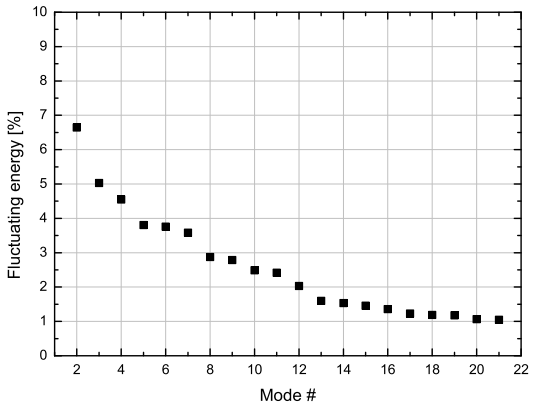

FIGURE 11. **Fluctuating kinetic energy distribution of first 20 modes**

cies goes up to 41000 [Hz] with a resolution of 245 [Hz]. Modes 2 and 3 reveal an almost coincident spectrum showing a clear peak at 24800 [Hz], as shown in Fig.12. The same analysis conducted for modes 4 and 5 highlights the same parallel behavior of the coupled modes and shows a more spread spectrum with excited frequencies ranging between 15000 and 28000 [Hz]. Those values report that the characteristic frequencies of the jet and of the acoustic forcing are largely separated thus the hypothesis of flow field independence from the sinusoidal pressure waves is confirmed. As a matter of fact the flow field in the acoustic simulation (not shown here for the sake of brevity) is reproducing the same modes as in the natural jet and most of the unsteady effects at the investigated frequencies are connected with the temporal coefficients of the first mode representing a waving mean velocity.

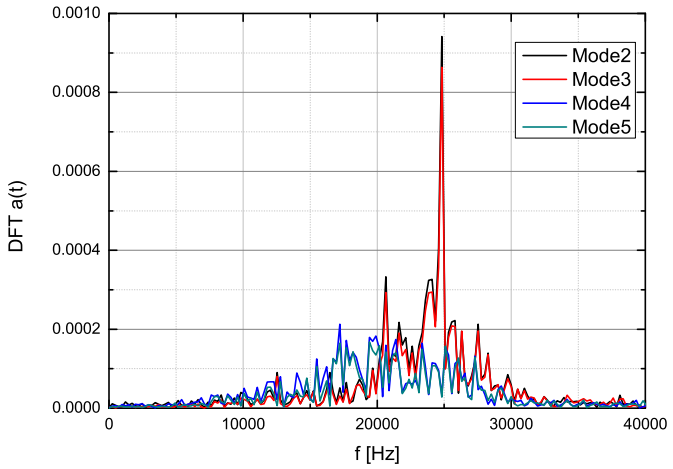

FIGURE 12. **Discrete Fourier Transform of first 4 pressure modes**

The natural frequencies of these first modes are hence pretty far from the investigated frequency range allowing the assumption of independence of such modes from the acoustic forcing.

CONCLUSIONS

In next lean burn aero-engine combustors the onset of thermo-acoustic oscillation is probably the major design issue; to mitigate pressure fluctuations, damping characteristics of multi-perforation used to cool liner walls may have great potentialities.

For this purpose, an assessment of numerical models used to predict the acoustic behavior of multi-perforated liners was performed. The presented methodologies offer an increasing order of complexity.

First of all a 1D network tool based on linear acoustics and the wall compliance concept introduced by Howe is considered. Secondly a FEM approach with a specific wall compliance to replicate the effect of multi-perforation was used to obtain a 2D reconstruction of pressure field in presence of a background mean flowfield. Finally LES simulations were performed within an open-source toolbox reconstructing the full unsteady turbulent structures.

A well-known literature test-case was considered to validate the three methodologies reporting a fairly good agreement in terms of absorption coefficient.

The three models was then used to explore different geometries of multi-perforated cylindrical liners. In particular a wide test matrix with 9 different geometries and various fluidynamic parameters, obtained by typical engine working conditions, was investigated with the 1D network tool. The model was able to quickly catch, at different frequencies, the dependence of acoustic absorption coefficient from the holes inclination angle, diameter and overall porosity, reporting a proper physical sensitivity to grazing and bias flows Mach number.

A selected case of the explored test matrix was then studied through FEM and LES models, obtaining a quite good agreement with 1D network approach in terms of absorption coefficient levels at various exciting frequencies. FEM and LES formulations were then used to explore the effect of in-line or staggered holes perforation, which is not accounted for in the 1D model.

Finally, in order to have a deeper comprehension of the flow structures through which acoustic energy is dissipated, a detailed analysis of naturally excited jet was performed: this type of investigation results very useful since the investigated range of forcing largely reside in the linear regime, as long as the selected frequencies are far from those associated with the natural modes of the jet.

This study has revealed the possible convenience of using all the three selected methodologies at different phases of the design flow. The very low pre-processing and computational costs of the 1D network tool allows to quick select the optimal liner porosity in the preliminary steps, while LES simulations would allow to investigate with high accuracy the fluidynamic details of the damping process. The FEM methodology, combined with a proper sub-models (wall compliance, flame transfer function), can be conveniently used to analyze the overall thermoacoustic behavior of the combustor.

This work represents a first step of a longer experimental-numerical research activity regarding the two-fold optimization (cooling-acoustic damping) of multi-perforated liners for lean burn combustors. In particular an experimental survey is being carried out in order to evaluate the impedance of representative combustor liners geometries. The same geometries will be finally investigated in terms of film cooling effectiveness so as to define thermal-acoustics best design practices.

ACKNOWLEDGMENTS

The reported work was performed within the European research project *Knowledge for Ignition, Acoustic, and Instabilities - KIAI* (RTD-Project 7^{th} FP, Contract No. 211843) The permission for the publication is gratefully acknowledged by the authors.

REFERENCES

[1] T.C. Lieuwen, V. Yang, 2005. *Combustion Instabilities in Gas Turbine Engines. Operational Experience, Fundamental Mechanisms and Modeling*. AIAA.

[2] A.P. Dowling, 1995. "The calculation of thermoacoustic oscillations". *Journal of Sound and Vibrations*, **180**, pp. 557–581.

[3] Arcangeli, L., Facchini, B., Surace, M., and Tarchi, L., 2008. "Correlative analysis of effusion cooling systems". *ASME Journal of Turbomachinery*, **130**.

[4] Ceccherini, A., Facchini, B., Tarchi, L., Toni, L., and Coutandin, D., 2009. "Combined effect of slot injection, effusion array and dilution hole on the cooling performance of a real combustor liner". *ASME Turbo Expo*(GT2009-60047).

[5] Howe, M. S., 1979. "On the theory of unsteady high Reynolds number flow through a circular aperture". *Proceedings of the Royal Society of London*, **366**, pp. 205–223.

[6] Heuwinkel, C., Enghardt, L., Bake, F., Sadig, S., and Gerendas, M., 2010. "Establishment of a high quality database for the modelling of perforated liners". *ASME Turbo Expo*(GT2010-22329).

[7] Bhayaraju, U., Schmidt, J., Kashinath, K., and Hochgreb, S., 2010. "Effect of cooling liner on acoustic energy absorption and flame response". *ASME Turbo Expo*(GT2010-22616).

[8] Pankiewitz, C., and Sattelmayer, T., 2003. "Time domain simulation of combustion instabilities in annular combustors". *Journal of Engineering for Gas Turbines and Power*, **125**, pp. 677–685.

[9] Campa, G., and Camporeale, S., 2010. "Influence of flame and burner transfer matrix on thermoacoustic combustion instability modes and frequencies". *ASME Turbo Expo*(GT2010-23104).

[10] Martin, C., Benoit, L., Nicoud, F., and Poinsot, T., 2004. "Analysis of acoustic energy and modes in a turbulent swirled combustor". *Center for Turbulence Research Proceedings of the Summer Program*.

[11] Mendez, S., and Eldredge, J. D., 2009. "Acoustic modeling of perforated plates with bias flow for large-eddy simulations". *Journal of Computational Physics*, **228**, pp. 4757–4772.

[12] Eldredge, J. D., Bodony, D. J., and Shoeybi, M., 2007. "Numerical investigation of the acoustic behavior of a multi-perforated liner". *13th AIAA/CEAS Aeroacustic Conference*(3683).

[13] Andreini, A., Facchini, B., Mangani, L., and Simonetti, F., 2008. "Development and validation of a 1-D tool for thermoacoustic instabilities analysis in gas turbine combustors". *ASME Turbo Expo*(GT2008-51248).

[14] Eldredge, J., and Dowling, A., 2003. "The absorption of axial acoustic waves by a perforated liner with bias flow".

Journal of Fluid Mechanics, **485**, pp. 307–335.

[15] Luong, T., Howe, M., and McGowan, R., 2005. "On the Rayleigh conductivity of a bias-flow aperture". *Journal of Fluids and Structures*, **21**, pp. 769–778.

[16] Leppington, F., 1977. "The effective compliance of perforated screens". *Mathematika*, **24**, pp. 199–215.

[17] Hughes, I., and Dowling, A., 1990. "The absorption of sound by perforated linings". *Journal of Fluid Mechanics*, **218**, pp. 299–335.

[18] Leppington, F., and Levine, H., 1973. "Reflexion and transmission at a plane screen with periodically arranged circular or elliptical apertures". *Journal of Fluid Mechanics*, **61**, pp. 109–127.

[19] Hu, F., Li, X., and Lin, D., 2008. "Absorbing boundary conditions for nonlinear Euler and Navier-Stokes equations based on the perfectly matched layer technique". *Journal of Computational Physics*, **227**, pp. 4398–4424.

[20] Hu, F., 2005. "A perfectly matched layer absorbing boundary condition for linearized Euler equations with a non-uniform mean flow". *Journal of Computational Physics*, **208**, pp. 469–492.

[21] Weller, H. G., Tabor, G., Jasak, H., and Fureby, C., 1998. "A tensorial approach to computational continuum mechanics using object-oriented techniques". *Computers in Physics*, **12**(6).

[22] Fureby, C., Weller, H. G., Tabor, G., and Gosman, A. D., 1997. "A comparative study of subgrid scale models in homogeneous isotropic turbulence". *Physics of Fluids*, **9**(5), pp. 1416–1429.

[23] Fureby, C., 1996. "On subgrid scale modeling in large eddy simulations of compressible fluid flow". *Physics of Fluids*, **8**(5), pp. 1300–1311.

[24] Nicoud, F., and Ducros, F., 1999. "Subgrid-scale stress modelling based on the square of the velocity gradient tensor". *Flow, Turbulence and Combustion*, **62**, pp. 183–200.

[25] Poinsot, T. J., and Lele, S. K., 1992. "Boundary conditions for direct simulations of compressible viscous flows". *Journal of Computational Physics*, **101**, pp. 104–129.

[26] Jang, S. H., and Ih, J. G., 1998. "On the multiple microphone method for measuring in-duct acoustic properties in the presence of mean flow". *Journal of Acoustical Society of America*, **103**(3), pp. 1520–1526.

[27] Berkooz, G., Holmes, P., and Lumley, L. J., 1993. "The proper orthogonal decomposition in the analysis of turbulent flows". *Annual Review of Fluid Mechanics*, **25**, pp. 539–575.

[28] Thurow, B. S., and Lynch, K. P. "3D POD analysis of a naturally excited jet". *38th Fluid Dynamics Conference and Exhibit*(AIAA2008-4067).

[29] Rupp, J., Carrotte, J., and Spencer, A., 2010. "Methodology to identify the unsteady flow field associated with the loss of acoustic energy in the vicinity of circular holes". *ASME Turbo Expo 2010: Power for Land, Sea and Air*(GT2010-22178).

[30] Sirovich, L., 1987. "Turbulence and the dynamic of coherent structures, Part I: Coherent structures". *Quarterly of Applied Mathematics*, **45**, pp. 561–571.

[31] Bellucci, V., Paschereit, C. O., and Flohr, P., 2004. "Numerical and experimental study of acoustic damping generated by perforated screens". *AIAA Journal*, **42**(8), pp. 1543–1549.

[32] Liu, N., Hanjalic, K., Borello, D., and Tao, Z., 2009. "Large-eddy simulation of periodic discrete-hole effusion without and with rotation". *8th European Turbomachinery Conference*.

[33] Mendez, S., and Nicoud, F., 2008. "Large-eddy simulation of a bi-periodic turbulent flow with effusion". *Journal of Fluid Mechanics*, **598**, pp. 27–65.